Available on CMS information server

CMS AN -2010/349

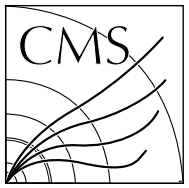

The Compact Muon Solenoid Experiment

Analysis Note

The content of this note is intended for CMS internal use and distribution only

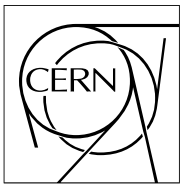

03 November 2010

Electron Efficiency Measurements with 2.88 pb^{-1} of pp Collision Data at $\sqrt{s} = 7$ TeV

Jeffrey Berryhill, Kalanand Mishra
Fermilab, Batavia, IL, USA

Georgios Daskalakis,
NCSR, Greece

Valerie Halyo, , Jeremy Werner
Princeton University, Princeton, NJ, USA

Si Xie
MIT, Cambridge, MA, USA.

Abstract

We present the first data driven electron efficiency measurements performed at CMS. These measurements were performed as part of the W/Z analysis, and use 2.88 pb^{-1} of pp collision data at $\sqrt{s} = 7$ TeV.

The Compact Muon Solenoid Experiment
CMS Draft Note
Mailing address: CMS CERN, CH-1211 GENEVA 23, Switzerland

tags

Electron Efficiency Measurements with 2.88 pb^{-1} of pp Collision Data at $\sqrt{s} = 7$ TeV

Jeffrey Berryhill[1], Georgios Daskalakis[2], Valerie Halyo[3], Kalanand Mishra[1], Jeremy Werner[3], and Si Xie[4]

[1] Fermilab, Batavia, IL, USA
[2] NCSR, Greece
[3] Princeton University, USA
[4] MIT, USA

Abstract

We present the first data driven electron efficiency measurements performed at CMS. These measurements were performed as part of the W/Z analysis, and use 2.88 pb^{-1} of pp collision data at $\sqrt{s} = 7$ TeV.

Contents

1 Motivation

Electron efficiency measurements are a central component of any physics analysis with electrons in the final state. The purpose of this note is to briefly describe the techniques and results of the electron efficiency measurements for the W and Z cross section measurements of CMS AN-264/2010 [1]. We describe the tag and probe methodology used with 2 alternative signal shape hypotheses. All relevant systematics are evaluated, and the results are detailed in multiple tables and plots. These efficiency measurements, along with the cross section measurements of CMS AN-264/2010, were performed on a dataset corresponding to an integrated luminosity of 2.88 pb^{-1} of pp collisions at $\sqrt{s} = 7$ TeV. This data was collected at the CMS detector between March 30 - Aug 30, 2010, including runs 132440-144114.

2 Introduction to Tag and Probe Methodology

The tag and probe method for computing electron efficiencies leverages Z→ee decays as a high-purity source of unbiased electrons from which to extract efficiencies. The so called *tag* electron is the control electron to which stringent electron selection criteria is applied. The *probe* electron, on the other hand, is the test electron having selection criteria according to the efficiency under study. Naturally, imposing an invariant mass cut on the tag-probe pair, about the Z→ee peak ensures a high purity sample of tag-probe pairs. This method is well documented, for instance, in CMS AN-2009/111 [2].

After constructing the tag criteria and the probe criteria for the specific efficiency under study, 2 samples then arise: Events with 1 tag electron and 1 probe electron passing the particular selection requirements under study (Tag+Pass), and events with a tag electron and a probe failing the selection requirement under study (Tag+Fail). The efficiency calculation then reduces to an estimation of the signal yield in the passing and failing samples. In the present analysis this estimation is carried out via simultaneous maximum likelihood fits to the dielectron invariant mass distributions in the 2 samples.

For the W and Z cross section measurement, the efficiency calculation is broken down into 3 steps:

- Super Cluster (SC) to Gaussian Sum Filter track-matched electron (Reco),
- Reco to the working point 80% selection criteria (WP80),
- WP80 to the online trigger requirement (HLT).

Since the electron selection and background levels are different for electrons in the ECAL barrel and ECAL endcap, efficiencies are measured separately for barrel and endcap. Due to possible correlations between electron selection efficiency and the level of misalignment between the tracker and the ECAL, the efficiency may have residual charge dependence. Therefore the measurement is performed separately for electrons and positrons [1].

[1] Since for the SC→Reco step the probe has no associated charge, its charge is taken to be the opposite of that of the tag.

3 Event Selection

3.1 Acceptance

We require both electrons from Z→ee decays to be within the ECAL fiducial area, *i.e.*, within $|\eta| < 2.5$, but excluding $1.4442 < |\eta| < 1.560$. Both electrons should have super cluster $E_T > 20$ GeV (after applying energy scale correction). Additionally, the dielectron invariant mass should be close to the nominal Z mass: $60 < M_{ee} < 120$ GeV. The choice of this mass window is driven by two considerations:
(1) it should be consistent as much as possible with our Z cross section measurement window, and
(2) it should be sufficiently generous that failing probes do not appreciably fall outside the mass window.

3.2 Working Point 80% Selection Criteria

We list the criteria used to defined Working Point 80% selection in Table 1. Please note that in ECAL isolation computation, a 1 GeV pedestal subtraction is NOT used. The electron E_T is used after correcting for the ECAL energy scale: 1.015 ± 0.002 in barrel and 1.03 ± 0.005 in endcaps. However, no such correction is applied to the denominator of H/E. We assume an electron to be from conversion photon if both the angular distance of the partner track and the $\Delta\cot\theta$ of the partner track are less than 0.02. In other words, if an electron satisfies BOTH these criteria then it does not pass Working Point 80% selection. In order to compute these partner track variables we assume magnetic field inside the tracking detector to be 3.8 T uniform.

Variables	Selection in Barrel	Selection in Endcaps
Missing hits in inner pixel layers	$= 0$	$= 0$
Distance of the partner track	> 0.02	> 0.02
$\Delta\cot\theta$ of the partner track	> 0.02	> 0.02
Track isolation in dR=0.3 / electron E_T	< 0.09	< 0.04
ECAL isolation in dR=0.3 / electron E_T	< 0.07	< 0.05
HCAL isolation in dR=0.3 / electron E_T	< 0.10	< 0.025
Shower shape: $\sigma_{i\eta i\eta}$	< 0.01	< 0.03
Track-super cluster matching: $\lvert\Delta\phi\rvert$	< 0.06	< 0.03
Track-super cluster matching: $\lvert\Delta\eta\rvert$	< 0.004	–
H/E	< 0.04	< 0.025

Table 1: List of Working Point 80% Selection Criteria.

3.3 Trigger Selection

We use unprescaled single electron trigger with the lowest p_T threshold. Table 2 shows the list of triggers used for each data-taking period.

Run range	HLT trigger path used	L1 trigger
132440–137028	HLT_Photon10_L1R (with trigger object $E_T > 15$ GeV)	L1_SingleEG5
138564–140401	HLT_Photon15_Cleaned_L1R	L1_SingleEG5
141956–144114	HLT_Ele15_SW_CaloEleId_L1R	L1_SingleEG5

Table 2: List of electron triggers used for each data-taking period.

3.4 Candidate Selections

Following are the definitions of *tag*, *probe*, and *passing probe* in each efficiency step:

3.4.1 Super Cluster to Reco efficiency

Tag: *GsfElectron* passing working point 80% selection criteria
Probe: Super cluster
Passing probe: Super cluster matched to a reconstructed *GsfElectron* in the event.

The Tag+Fail sample has a huge background from QCD dijet events in presence of a small signal ($S/B << 1$). This makes it hard to reliably estimate the number of signal events in this sample. Therefore, we apply the following loose selection criteria to reduce the level of background: $H/E < 0.15(0.07)$ and $\sigma_{i\eta i\eta} < 0.01(0.03)$ for probe super clusters in the barrel (endcaps) of the electromagnetic calorimeter. These selections are fully efficient for signal events in Monte Carlo. We take any bias introduced by them as a source of systematic uncertainty, as we will describe later in this note. Note also for this step that since the probe has no associated charge, its charge is taken to be the opposite of that of the tag for the purpose of calculating the charge dependent efficiencies.

3.4.2 Reco to WP80 efficiency

Tag: *GsfElectron* passing working point 80% selection criteria
Probe: *GsfElectron*
Passing probe: *GsfElectron* passing WP80 criteria.

3.4.3 WP80 to the online trigger requirement efficiency

Tag: *GsfElectron* passing working point 80% selection criteria
Probe: *GsfElectron* passing working point 80% selection criteria
Passing probe: *GsfElectron* passing WP80 criteria and matched to an online trigger object that fired the unprescaled single electron trigger with the lowest E_T threshold.

Note that in a few extreme cases for this step there are only just a few events in the Tag+Fail sample and so we are limited to just counting them, assuming they all are signal.

3.5 Arbitration in Case of Multiple Candidates

After applying dielectron invariant mass cut some events are left with more than one Z candidate [1]. In case there are more than one Z candidates to choose from, we make the following arbitration. We consider only those events which have at least one tag candidate.

- If there are two probe candidates in the event and if only one of them also passes the tag criteria then choose the one which passes the tag criteria.
- If there are two probe candidates in the event and if both pass the tag criteria then choose one of them randomly.

[1] This happens with a frequency of several percent for *Tag+SuperCluster* combination, a few percent for *Tag+GsfElectron* combination, and much less than a percent for tighter selections. Since we require *tag* electron to be of sufficiently good quality, it is rare to find more than one Z candidate in the event if *probe* electron is also required to be well identified.

- If there are two probe candidates in the event and if both fail the tag criteria then choose one of them randomly.
- If there are more than two probe candidates in the event then reject that event from consideration (*i.e.,* the event is dropped from both numerator and denominator).

In the efficiency calculation described in the following section we count the number of tag+probe permutations from Z decay in both numerator and denominator. Thus, events where both electrons pass *tag* criteria contribute twice in numerator and in denominator (assuming that the *tag* criteria are tighter than the *passingProbe* criteria).

4 Extraction of Efficiency and Signal Yields

In order to extract the signal components of the Tag+Pass and Tag+Fail samples, an unbinned maximum likelihood fit is performed in the dielectron invariant mass variable with specific signal models described in sections 5.1 and 5.2, and an exponential background shape. The efficiency enters as an explicit fit parameter, such that correlations are taken into account in the efficiency uncertainties extracted from the fit. The floating parameters of the fit are listed below:

- N_{Signal} : number of signal Tag+Probe pairs,
- $N_{\text{Bkg}}^{\text{pass}}$: number of background Tag+Pass pairs,
- $N_{\text{Bkg}}^{\text{fail}}$: number of background Tag+Fail pairs,
- ϵ : efficiency,
- χ_{pass} : coefficient of the exponential background for the Tag+Pass sample,
- χ_{fail} : coefficient of the exponential background for the Tag+Fail sample.

The signal and background are extracted in the Tag+Pass and Tag+Fail samples through the following relations:

$$N^{\text{pass}}(\text{M}_{\text{ee}}) = N_{\text{Signal}} \cdot (\epsilon) \cdot P_{\text{Signal}}^{\text{pass}}(\text{M}_{\text{ee}}) + N_{\text{Bkg}}^{\text{pass}} \cdot P_{\text{Bkg}}^{\text{pass}}(\text{M}_{\text{ee}}) \quad (1)$$

$$N^{\text{fail}}(\text{M}_{\text{ee}}) = N_{\text{Signal}} \cdot (1-\epsilon) \cdot P_{\text{Signal}}^{\text{fail}}(\text{M}_{\text{ee}}) + N_{\text{Bkg}}^{\text{fail}} \cdot P_{\text{Bkg}}^{\text{fail}}(\text{M}_{\text{ee}}) \quad (2)$$

where $P_{\text{Signal}}^{\text{pass}}$ and $P_{\text{Signal}}^{\text{fail}}$ are the probability density functions in the dielectron invariant mass variable for the signal in the Tag+Pass and Tag+Fail samples, respectively. $P_{\text{Bkg}}^{\text{pass}}$ and $P_{\text{Bkg}}^{\text{fail}}$ are the probability density functions in the mass variable for the background and given by:

$$P_{\text{Bkg}}^{\text{pass}}(\text{M}_{\text{ee}}) \sim e^{-\chi_{\text{pass}}\text{M}_{\text{ee}}} \quad (3)$$

$$P_{\text{Bkg}}^{\text{fail}}(\text{M}_{\text{ee}}) \sim e^{-\chi_{\text{fail}}\text{M}_{\text{ee}}} \quad (4)$$

For the current results, the contribution of background in the Tag+Pass sample is very low, being less than 1% and consistent with 0 in the Reco→WP80 and WP80→HLT steps ([3] and [4]). Thus in order to avoid biasing the fit, we constrain the background in the Tag+Pass sample to be 0 for these steps [2].

[2]This is true only for our nominal fit where signal template is taken from a next-to-leading-order Monte Carlo generator-level shape convolved with suitable resolution model as described in section 5.2. For the purpose of cross check we also compute efficiency using an alternative signal template described in section 5.1. In the latter case, we let the background in the Tag+Pass sample to float.

5 Signal Shape Parametrization

5.1 Simulation Signal Shape With Additional Gaussian Smearing

In this approach, we construct the Tag+Pass and Tag+Fail mass shapes for the signal from the Monte Carlo simulation using the identical selection requirements that is used for data. In order to account for any effects not included in the simulation, we build the final signal shape probability density function by a convolution of the simulation line shape with an additional Gaussian resolution function. The width and mean of the Gaussian is allowed to float in the fit, accounting for an additional smearing to the simulation mass shape and a shift in the Z mass peak due to miscalibration of the energy scale.

5.2 Generator-Level Shape Convolved with a Resolution Model

One possible parametrization of the lineshape is to take the signal shape directly from the output of a next to leading order Monte-Carlo generator and then convolve it with some detector resolution model. This is what is done in this section. The generator shape is extracted directly from the POWHEG [5] Monte-Carlo generator. The resolution model is a Crystal-Ball modified to include an extra half Gaussian on the high end tail. This resolution model is purely empirical: Before data taking commmenced, it was observed to describe the detector simulation quite well and was later confirmed to also describe the data well. With 2.88 pb^{-1} of data, many of the bins we perform fits in are statistics limited. Therefore at the moment we must take a rather ad-hoc approach to which parameters of the line shape model we allow to float: To summarize, we allow as many parameters to float as possible under the constraints that the fit converges and MINOS [6] is still able to properly calculate the positive and negative uncertainties on each of the floating parameters. In addition to the evaluation of the MINOS uncertainties, detailed pull studies have also been performed so that the statistical features of this fit are thoroughly understood to be stable.

6 Systematic Uncertainties

6.1 Signal Shape Systematics

Due to the large amount of material associated with the tracker and its support structures that an electron must traverse before reaching the electromagnetic calorimeter, a relatively prominent low mass tail is present from bremstrahlung and energy loss. The precise behavior of this tail in the signal mass shape, particularly in the Tag+Fail sample, can significantly affect the results of the efficiency measurement fit. Due to the fact that this efficiency measurement has been performed on the prompt reconstruction data, whose alignment scenario is non-ideal, one is particularly worried about the existence of correlations between inefficiencies from selection cuts affected by misalignment and the shape of the signal mass in the low mass region. We attempt to constrain the shape of the low mass tail using data driven techniques.

2 different signal shape templates are selected from data, for the Tag+Fail sample. The first template is constructed from events where we require that the tag electron passes the very tight WP60 electron selection, and require that the missing transverse energy is less than 20.0 GeV in order to suppress W+Jet background. The probe is required to fail the nominal WP80 selection. The resulting mass shape is shown in Figure 1, compared with the shape extracted from the Monte Carlo simulation using the same selection. The second template is constructed from events where we require the usual WP80 electron selection for the tag electron, but require that the probe passes the WP95 isolation cuts and fails the remaining WP80 selection cuts. This

signal template is also shown in Figure 1. To extract systematic uncertainties due to the signal

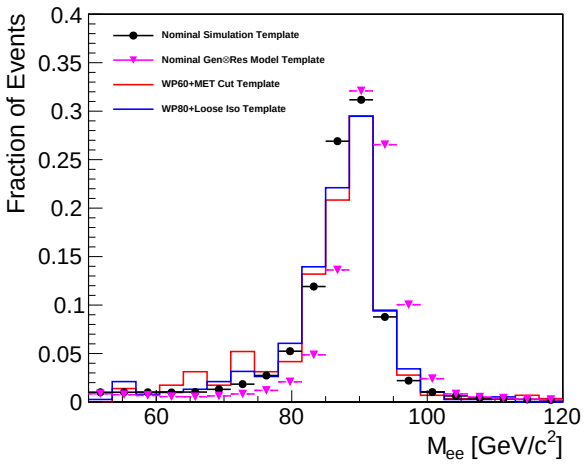

Figure 1: Comparison of nominal signal mass shape template from generator-level convolved with resolution model (solid triangles) and from simulation (solid circles) to templates extracted directly from data. We use two data-driven templates to estimate systematic uncertainty in efficiency. In one case (histogram in red color) we select events with *tag* electron passing the WP60 electron selection and a *probe* which fails the WP80 selection, and requiring that the missing transverse energy is less than 20.0 GeV. In the second case (histogram in blue color) we events with *tag* electron passing the WP80 electron selection and a *probe* which passes the WP95 isolation cuts but fails the WP80 selection.

shape, we perform the efficiency fit using these two fixed templates for the signal shape of the failing sample. The difference between the resulting efficiency measurement and the efficiency measured using the nominal method is taken as a systematic uncertainty. The results of this fit are shown in Figure 2 and 3 for the first and second template respectively. Table 3 summarizes the systematic uncertainties from this procedure. The systematic uncertainties in the endcap are artificially small due to the lack of any events in the mass sidebands in the Tag+Fail sample from tag and probe selection, simply due to the small sample size. A conservative systematic uncertainty of 2% is assigned to both the barrel and the endcap.

Data Based Signal Template	Barrel	Endcap
WP60 Tag + MetCut	1.8%	0.0%
WP80 Tag + Isolated Probe	1.0%	0.2%

Table 3: Systematic uncertainties obtained from the difference between the efficiency measurement using the data driven signal shape templates and the efficiency measured using the nominal signal shape model.

6.2 Background Shape Systematics

To estimate the systematic due to the background parametrization, large numbers of pseudo-experiments are generated with a background PDF of the form $1/M^{\alpha}$, where $\alpha = 5$. For each pseudoexperiment S/B is fixed to the level reported back by the fit to the data for each efficiency step. This pseudo Monte-Carlo is then fit back to the sum of the signal shape from whence it was generated and several background shape hypothesis, including an exponential decay, and a power law. The systematic uncertainty is then quoted as the maximal difference among the

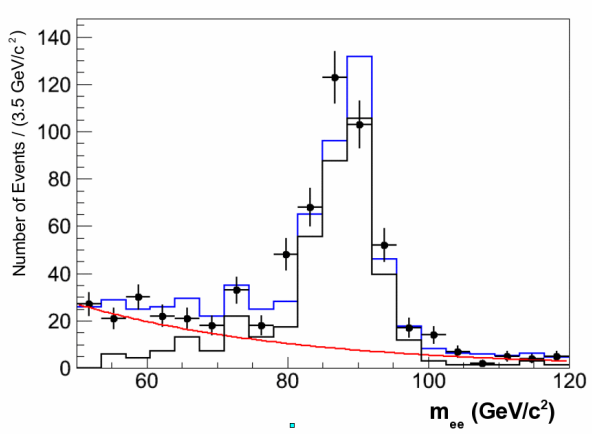

Figure 2: Fit result for the Tag+Fail sample, using the signal template constructed from selecting WP60 Tag electrons and requiring a missing transverse energy cut. The red curve indicated the fitted background, the black histogram is the fitted signal, and the blue histogram is the fit result for the signal plus background.

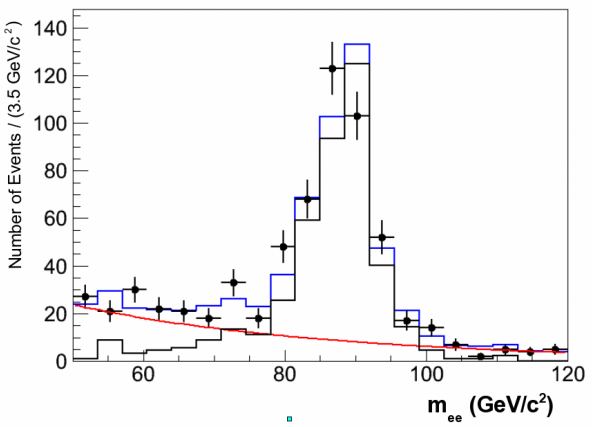

Figure 3: Fit result for the Tag+Fail sample, using the signal template constructed from selecting WP80 Tag electrons and requiring that the probe passes the WP95 isolation cuts. The red curve indicated the fitted background, the black histogram is the fitted signal, and the blue histogram is the fit result for the signal plus background.

remaining background hypotheses. The background systematics are found to be small, and are listed for each efficiency step in table 4.

6.3 Energy Scale Systematics

To estimate the systematic due to the uncertainty on the energy scale, the electron energies in the Monte-Carlo are shifted in both the positive and negative directions by the uncertainty on the scale. The maximal difference among the 3 extracted efficiency values (nominal, positive shift, negative shift) is then taken as the systematic for each step. The energy scale systematics are found to be quite small, and are listed for each efficiency step in table 5.

Table 4: The Background Parametrization Systematic Uncertainty for each Efficiency Step

Step	$\Delta\epsilon$
SC→Reco	0.0006
Reco→WP80	0.002
WP80→HLT	0.0000

Table 5: The Energy Scale Systematic Uncertainty for each Efficiency Step

Step	$\Delta\epsilon$
SC→Reco	0.001
Reco→WP80	0.002
WP80→HLT	0.001

Table 6: The SC→Reco Efficiencies

Topology	Monte-Carlo		Data				Data/Monte-Carlo
	ϵ	$\Delta\epsilon$	ϵ	$\Delta\epsilon$ (stat)	$\Delta\epsilon$ (syst)	$\Delta\epsilon$ (total)	
EB	0.9851	0.0002	0.986	0.005	0.012	0.013	1.001 ± 0.013
EE	0.9629	0.0004	0.962	0.008	0.012	0.015	0.999 ± 0.016
EB e^-	0.9854	0.0002	0.985	0.005	0.012	0.013	0.999 ± 0.013
EE e^-	0.9624	0.0004	0.967	0.002	0.012	0.012	1.005 ± 0.012
EB e^+	0.9849	0.0002	0.987 [a]	0.004	0.012	0.013	1.002 ± 0.012
EE e^+	0.9634	0.0004	0.951	0.003	0.012	0.012	0.987 ± 0.012

[a] A minor error was discovered for this fit in that the exponentially falling background shape flipped to instead be growing in the Tag+Fail sample. The fit was later constrained to prevent this and yielded the corrected result: $\epsilon = 0.989 \pm 0.006$ (stat). As the difference is negligible, the original result quoted in the table above has been retained throughout the analysis, though the corresponding plots in Figure 13 have been updated to the corrected fit.

Table 7: The Reco→WP80 Efficiencies

Topology	Monte-Carlo		Data				Data/Monte-Carlo
	ϵ	$\Delta\epsilon$	ϵ	$\Delta\epsilon$ (stat)	$\Delta\epsilon$ (syst)	$\Delta\epsilon$ (total)	
EB	0.8547	0.0004	0.791	0.018	0.020	0.027	0.925 ± 0.032
EE	0.7488	0.0006	0.692	0.020	0.020	0.028	0.924 ± 0.037
EB e^-	0.8545	0.0005	0.793	0.027	0.020	0.034	0.929 ± 0.040
EE e^-	0.7489	0.0009	0.701	0.038	0.020	0.043	0.936 ± 0.057
EB e^+	0.8549	0.0005	0.780	0.031	0.020	0.037	0.913 ± 0.044
EE e^+	0.7487	0.0009	0.701	0.029	0.020	0.035	0.936 ± 0.047

6.4 Results

In this section we provide the efficiency results using the generator-level line shape described in Section 5.2. These results are summarized in Tables 6 - 8, including all statistical and systematic uncertainties. The corresponding fit plots are provided in Appendix B. Results from the Monte-Carlo are also provided, and these were evaluated via simple cut-and-count on the Monte-Carlo truth. For comparison and cross check the results using the alternative simulation based signal shape model are summarized in Appendix A. The 2 approaches yield efficiencies that are in agreement to within the uncertainties.

Table 8: The WP80→HLT Efficiencies

Topology	Monte-Carlo		Data				Data/Monte-Carlo
	ϵ	$\Delta\epsilon$	ϵ	$\Delta\epsilon$ (stat)	$\Delta\epsilon$ (syst)	$\Delta\epsilon$ (total)	
EB	0.997	0.0001	0.989	0.003	0.001	0.0032	0.992 ± 0.003
EE	0.988	0.0003	0.992	0.005	0.001	0.0051	1.004 ± 0.005
EB e^-	0.997	0.0001	0.986	0.005	0.001	0.0051	0.989 ± 0.005
EE e^-	0.988	0.0004	0.994	0.006	0.001	0.0061	1.006 ± 0.006
EB e^+	0.996	0.0001	0.994	0.004	0.001	0.0042	0.998 ± 0.004
EE e^+	0.989	0.0004	0.990	0.007	0.001	0.0071	1.001 ± 0.007

7 Conclusions

We have presented the first electron efficiency measurements performed at CMS. These measurements were performed as part of the W and Z inclusive cross section measurements, and used 2.88 pb^{-1} of pp Collision Data at $\sqrt{s} = 7$ TeV. This note has summarized these measurements, described all of the associated systematic uncertainties.

References

[1] *Updated Measurements of Inclusive W and Z Cross Sections at 7 TeV*, CMS AN-2010/264.

[2] *Generic Tag and Probe Tool for Measuring Efficiency at CMS with Early Data*, CMS AN-2009/111.

[3] *Data Driven Techniques to Estimate the Background in the Z→ee Events*, CMS AN-2010/277.

[4] *Fake Lepton Background Estimate for the Z→ee Cross Section Measurement using the Fake Rate Method*, CMS AN-2010/284.

[5] *A New Method for Combining NLO QCD with Shower Monte Carlo Algorithms*, P. Nason, JHEP 0411, 040 (2004) [arXiv:hep-ph/0409146].

[6] D.Drijard, Statistical Methods in Experimental Physics, North-Holland, 1971.

A Simulation Based Signal Shape Fit Plots

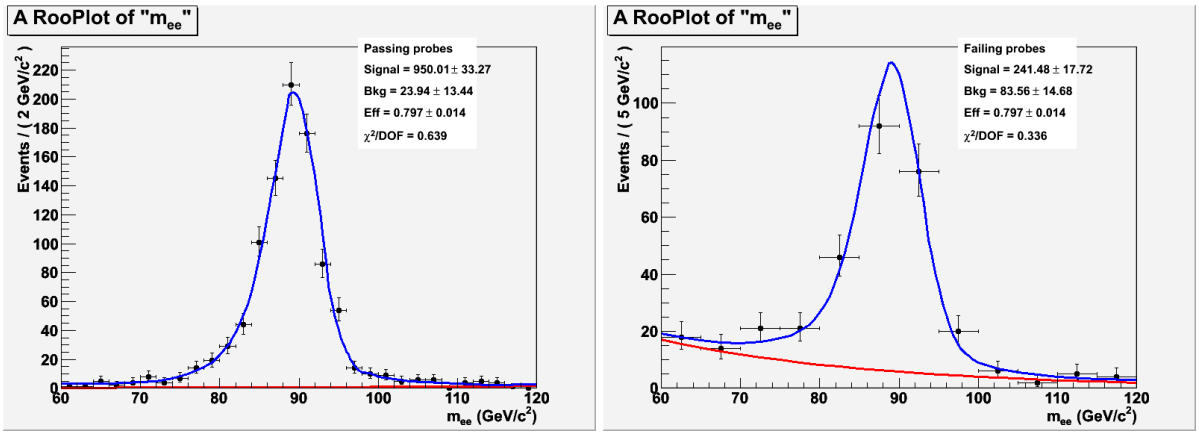

(a) (b)

Figure 4: The passing (a) and failing (b) fits for the Reco→WP80 step in the Ecal Barrel. The data is in black, background fit in red, and signal+background fit in blue.

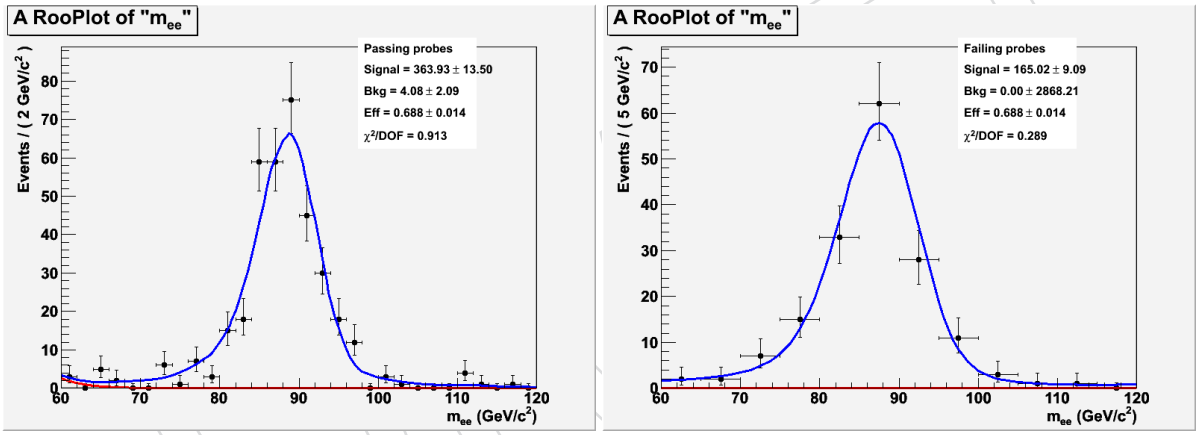

(a) (b)

Figure 5: The passing (a) and failing (b) fits for the Reco→WP80 step in the Ecal Endcap. The data is in black, background fit in red, and signal+background fit in blue.

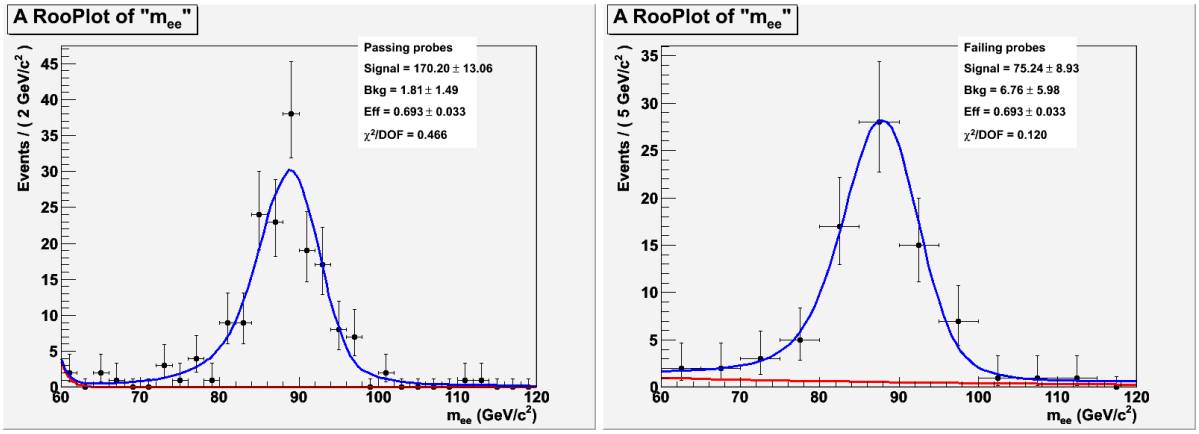

(a) (b)

Figure 6: The passing (a) and failing (b) fits for the Reco→WP80 step in the Ecal Barrel for electrons. The data is in black, background fit in red, and signal+background fit in blue.

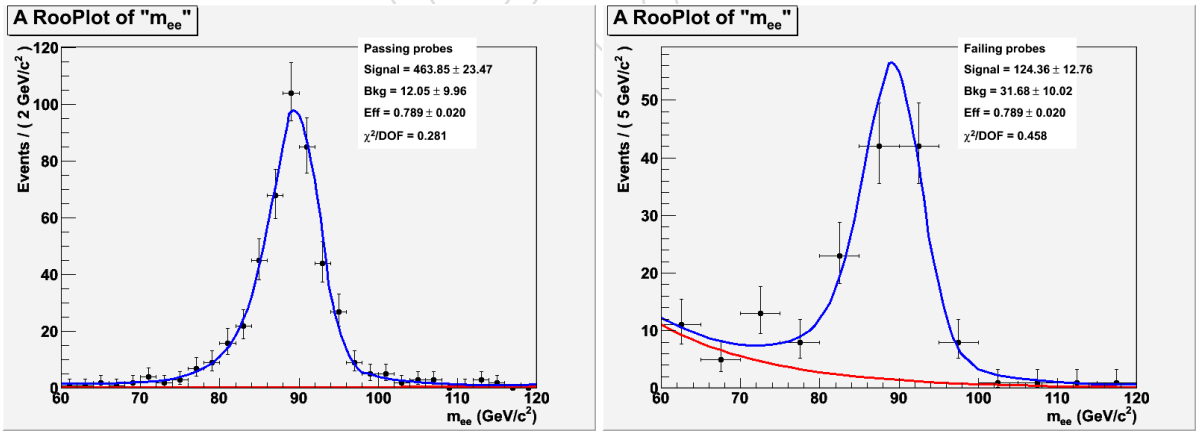

(a) (b)

Figure 7: The passing (a) and failing (b) fits for the Reco→WP80 step in the Ecal Barrel for positrons. The data is in black, background fit in red, and signal+background fit in blue.

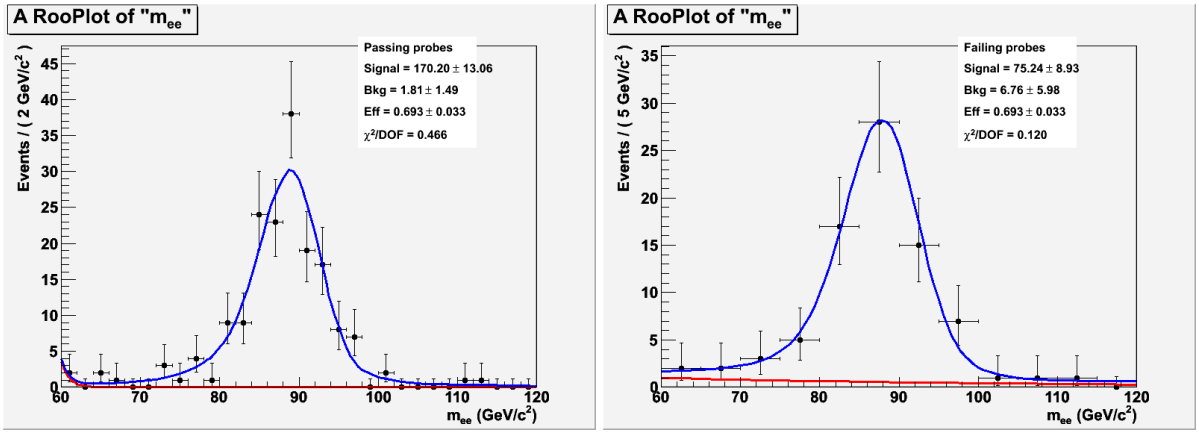

(a) (b)

Figure 8: The passing (a) and failing (b) fits for the Reco→WP80 step in the Ecal Endcap for electrons. The data is in black, background fit in red, and signal+background fit in blue.

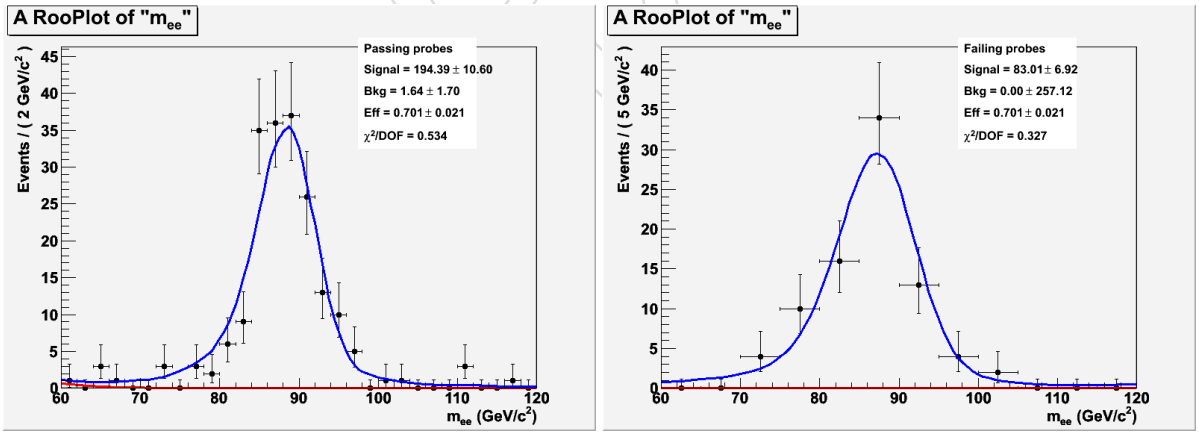

(a) (b)

Figure 9: The passing (a) and failing (b) fits for the Reco→WP80 step in the Ecal Endcap for positrons. The data is in black, background fit in red, and signal+background fit in blue.

B Generator-Level Signal Shape Fit Plots

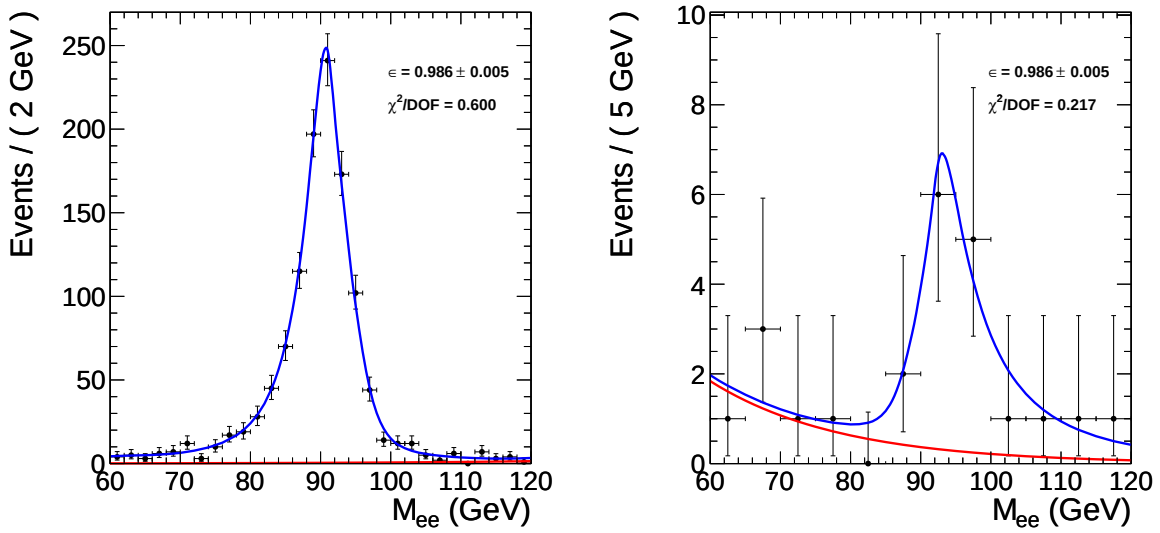

(a) (b)

Figure 10: The passing (a) and failing (b) fits for the SC→Reco step in the Ecal Barrel. The data is in black, background fit in red, and signal+background fit in blue.

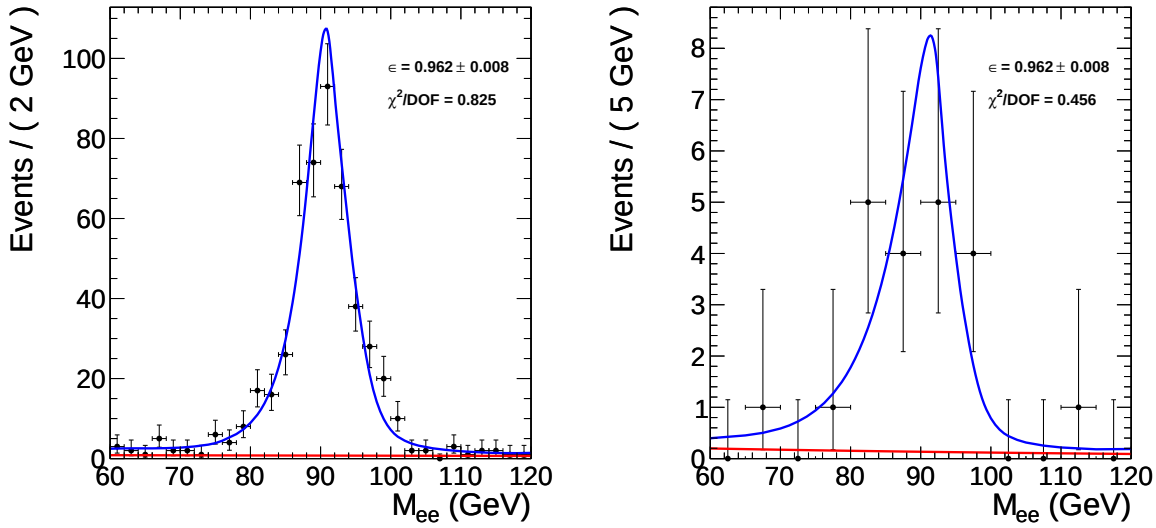

(a) (b)

Figure 11: The passing (a) and failing (b) fits for the SC→Reco step in the Ecal Endcap. The data is in black, background fit in red, and signal+background fit in blu e.

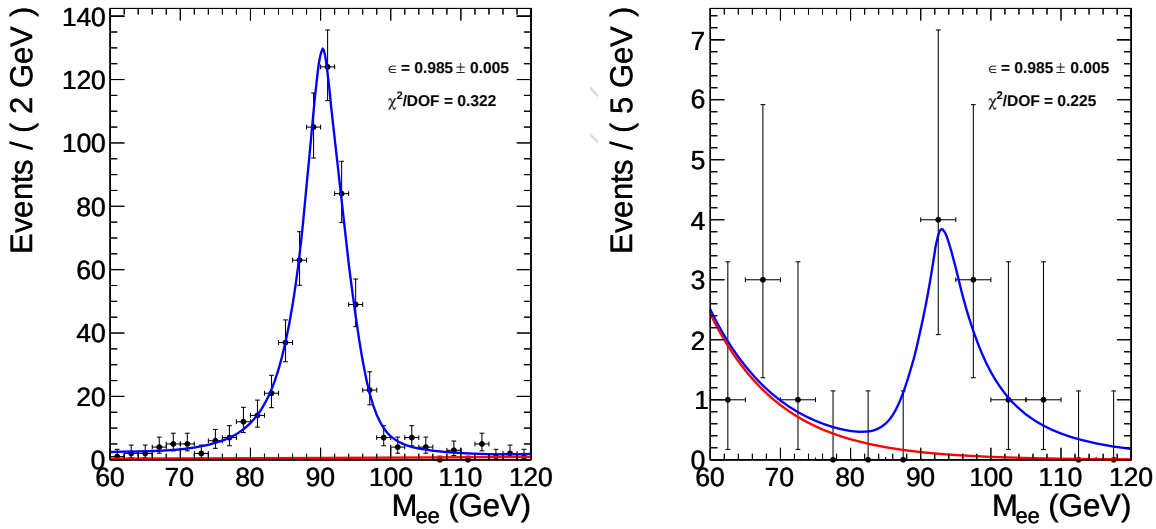

(a) (b)

Figure 12: The passing (a) and failing (b) fits for the SC→Reco step in the Ecal Barrel for electrons. The data is in black, background fit in red, and signal+background fit in blue.

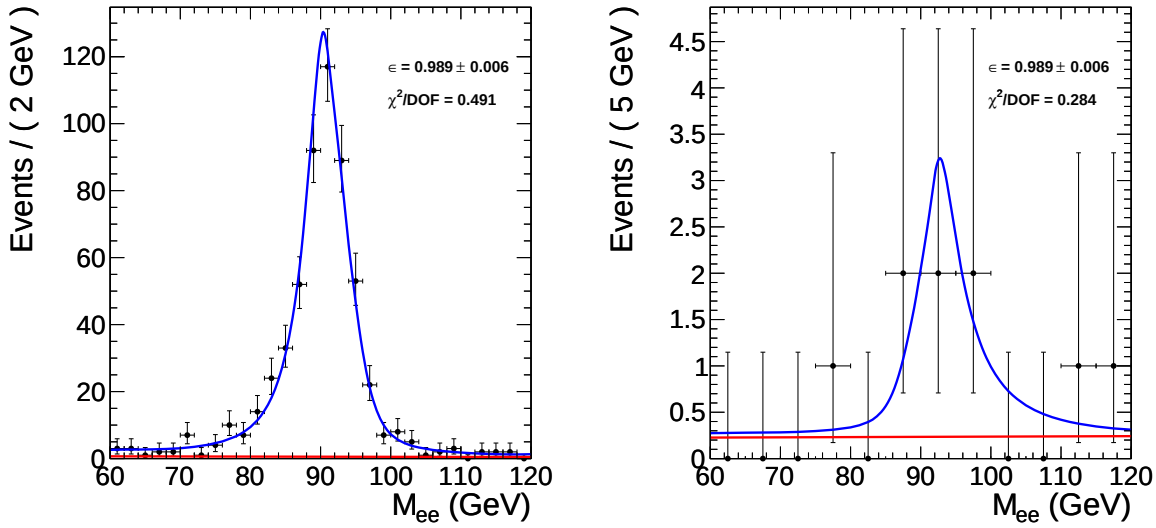

(a) (b)

Figure 13: The passing (a) and failing (b) fits for the SC→Reco step in the Ecal Barrel for positrons. The data is in black, background fit in red, and signal+background fit in blue.

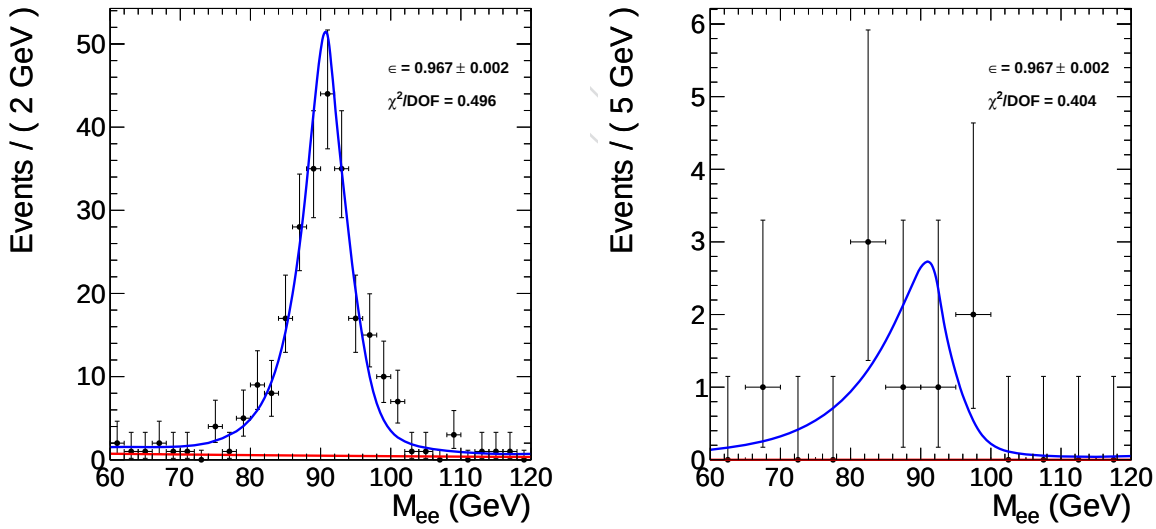

(a) (b)

Figure 14: The passing (a) and failing (b) fits for the SC→Reco step in the Ecal Endcap for electrons. The data is in black, background fit in red, and signal+background fit in blue.

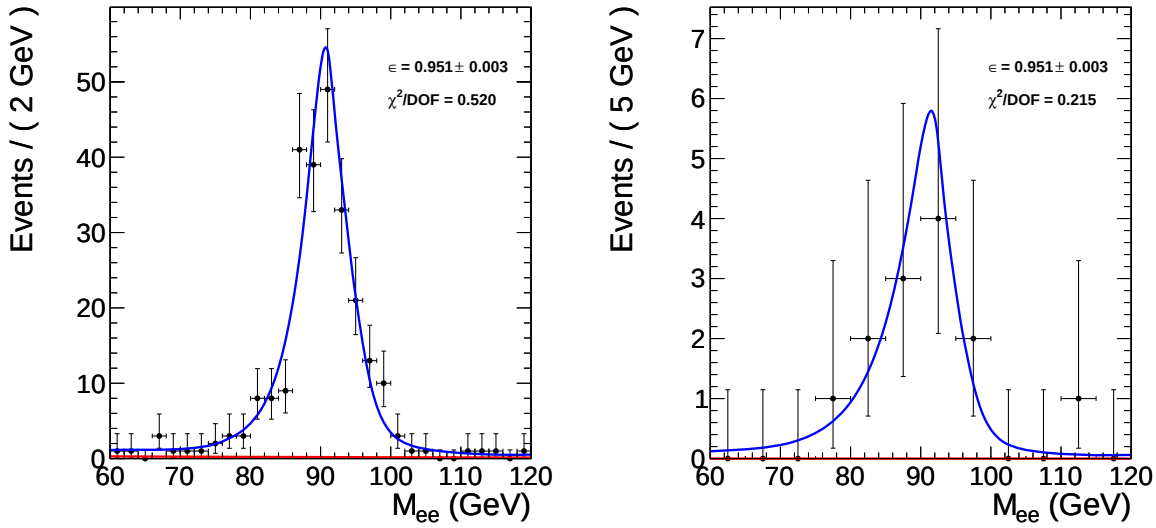

(a) (b)

Figure 15: The passing (a) and failing (b) fits for the SC→Reco step in the Ecal Endcap for positrons. The data is in black, background fit in red, and signal+background fit in blue.

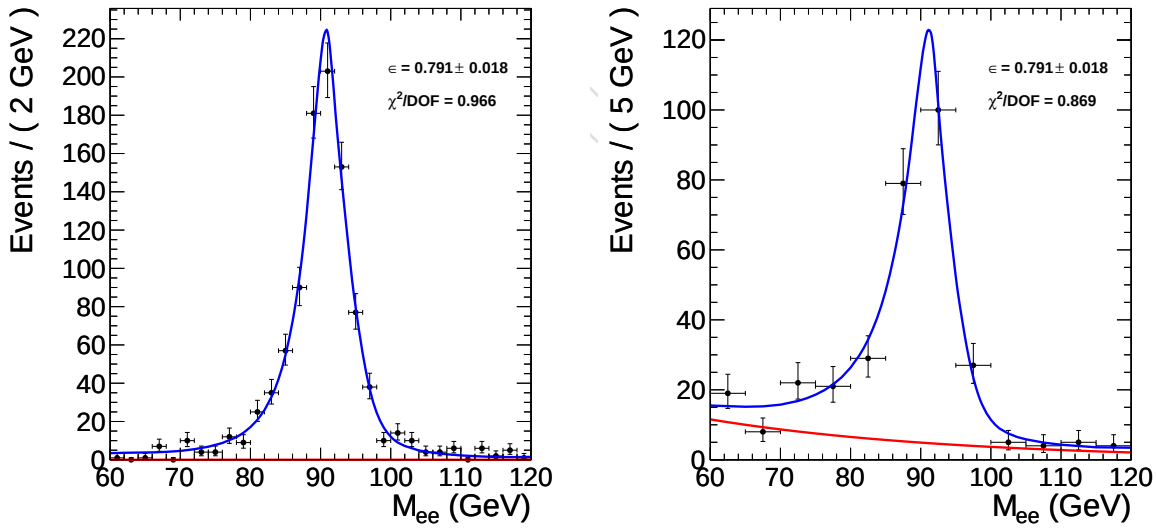

(a) (b)

Figure 16: The passing (a) and failing (b) fits for the Reco→WP80 step in the Ecal Barrel. The data is in black, background fit in red, and signal+background fit in blue.

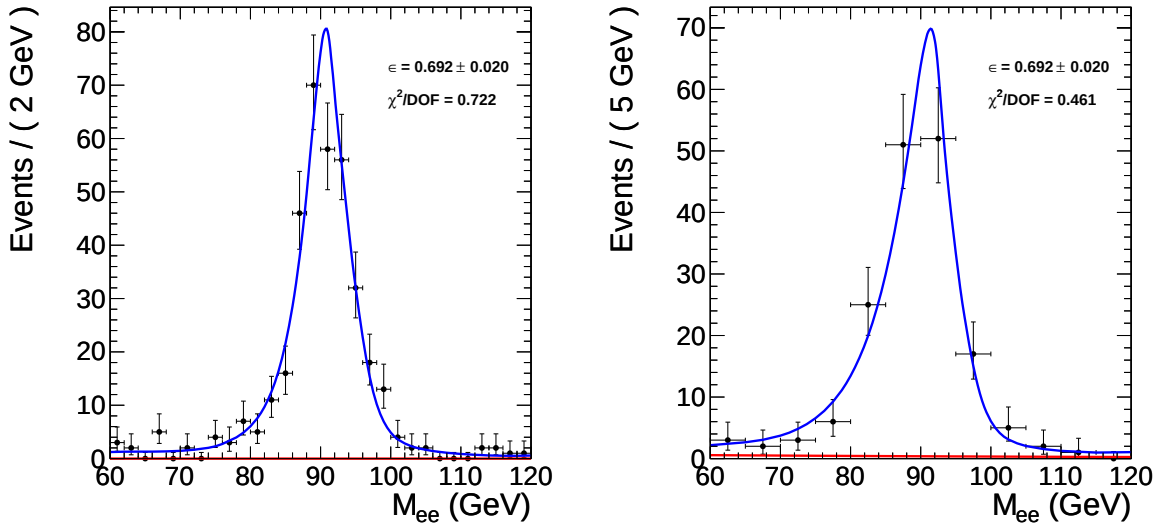

(a) (b)

Figure 17: The passing (a) and failing (b) fits for the Reco→WP80 step in the Ecal Endcap. The data is in black, background fit in red, and signal+background fit in blue.

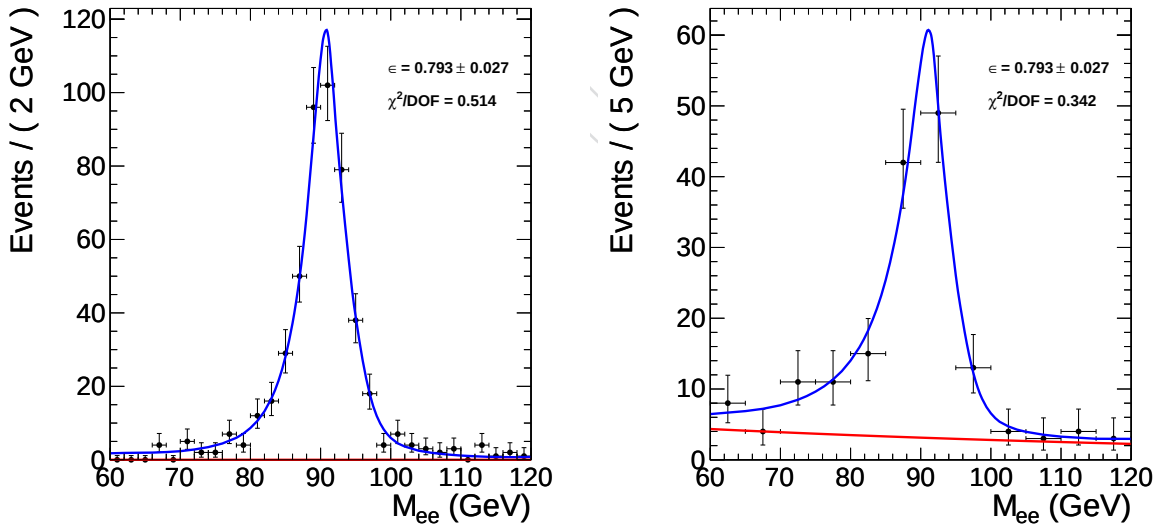

(a) (b)

Figure 18: The passing (a) and failing (b) fits for the Reco→WP80 step in the Ecal Barrel for electrons. The data is in black, background fit in red, and signal+background fit in blue.

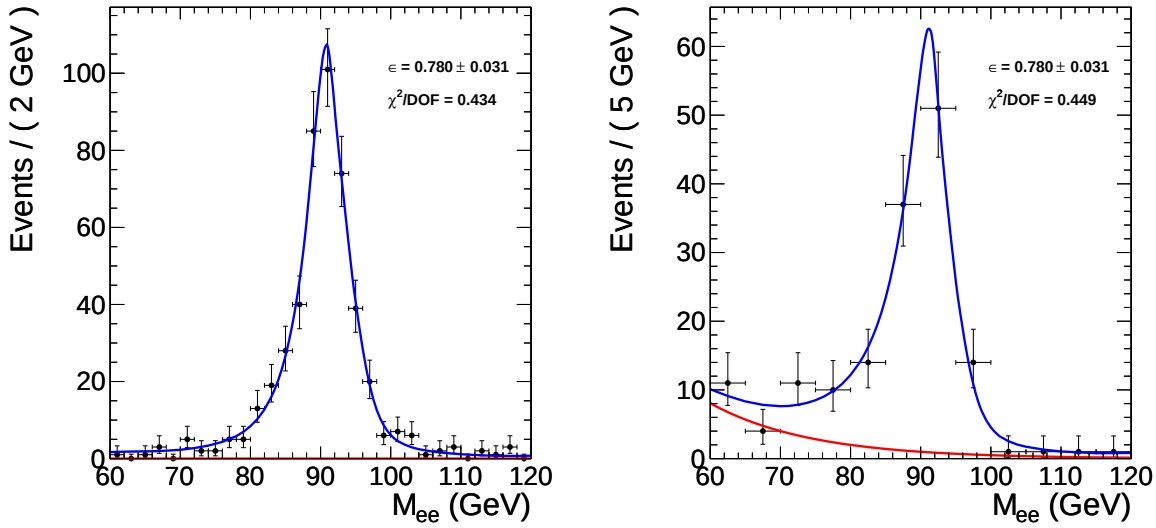

(a) (b)

Figure 19: The passing (a) and failing (b) fits for the Reco→WP80 step in the Ecal Barrel for positrons. The data is in black, background fit in red, and signal+background fit in blue.

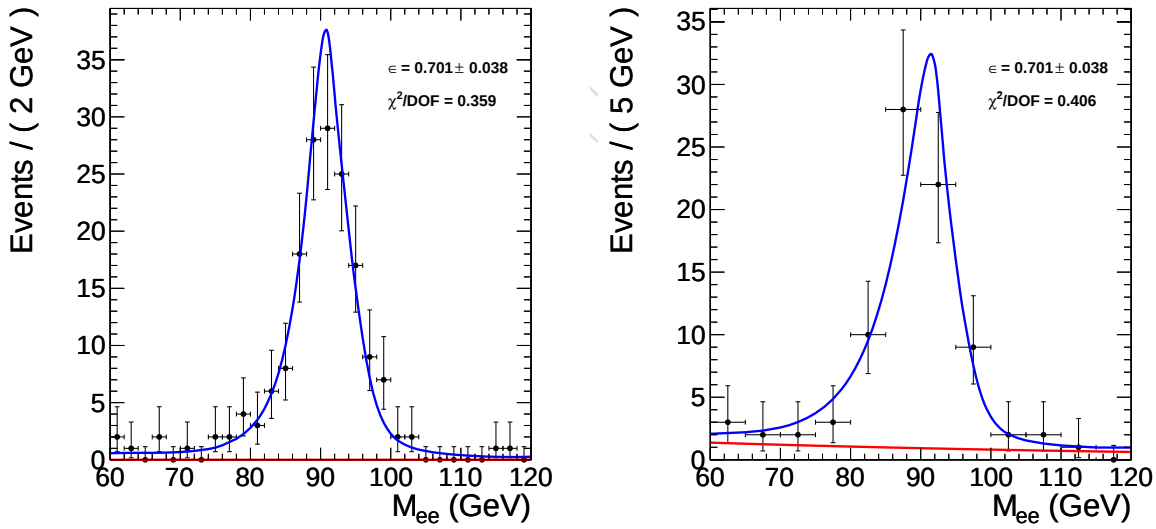

(a) (b)

Figure 20: The passing (a) and failing (b) fits for the Reco→WP80 step in the Ecal Endcap for electrons. The data is in black, background fit in red, and signal+background fit in blue.

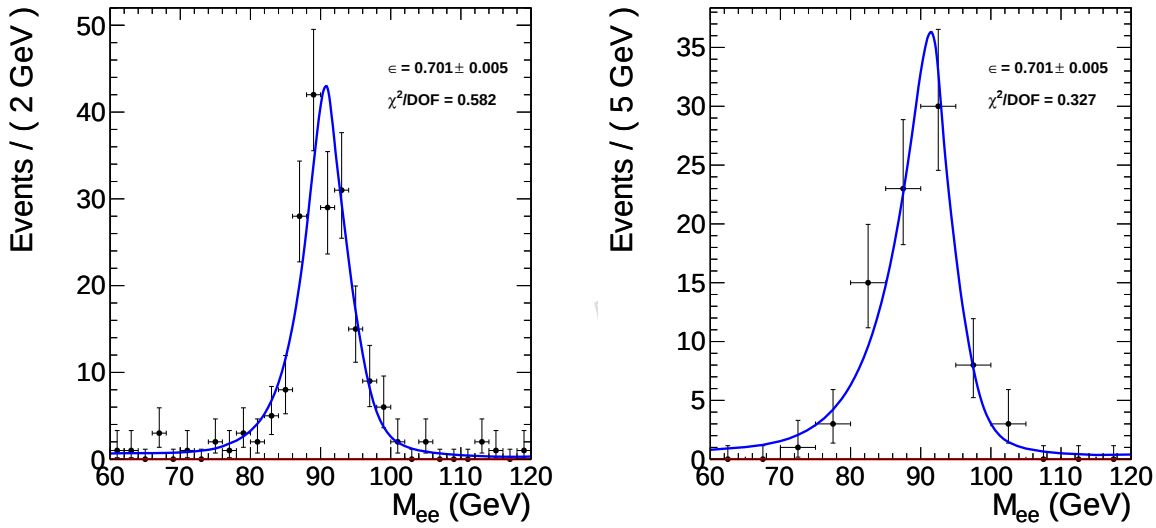

(a) (b)

Figure 21: The passing (a) and failing (b) fits for the Reco→WP80 step in the Ecal Endcap for positrons. The data is in black, background fit in red, and signal+background fit in blue.

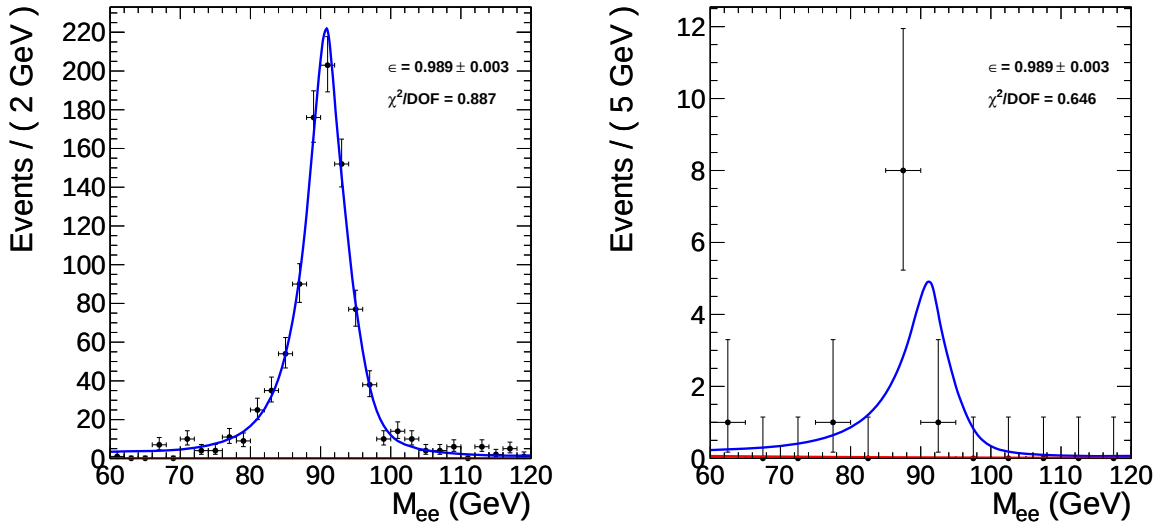

(a) (b)

Figure 22: The passing (a) and failing (b) fits for the WP80→HLT step in the Ecal Barrel. The data is in black, background fit in red, and signal+background fit in blue.

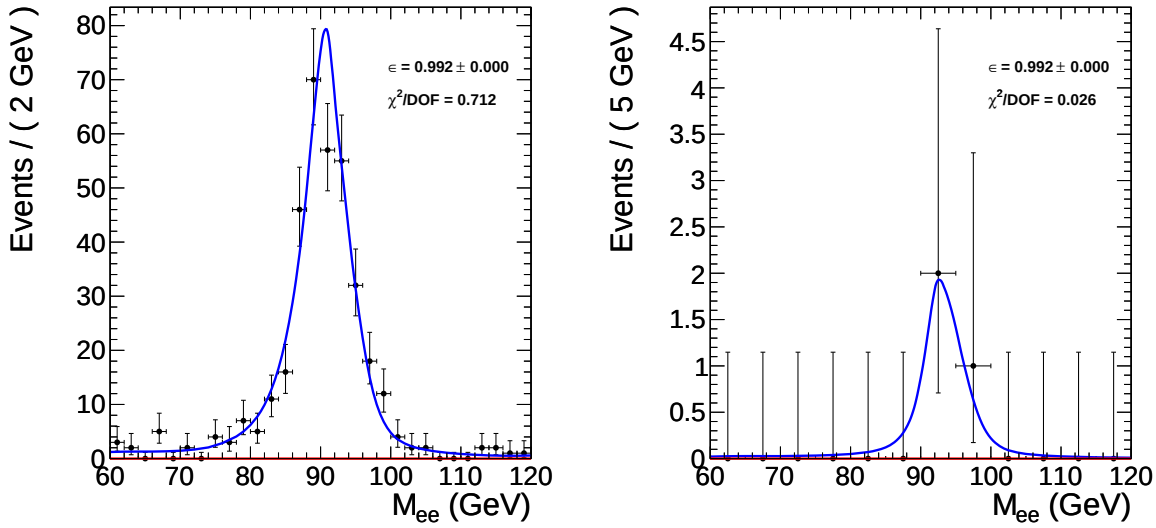

(a) (b)

Figure 23: The passing (a) and failing (b) fits for the WP80→HLT step in the Ecal Endcap. The data is in black, background fit in red, and signal+background fit in blue.

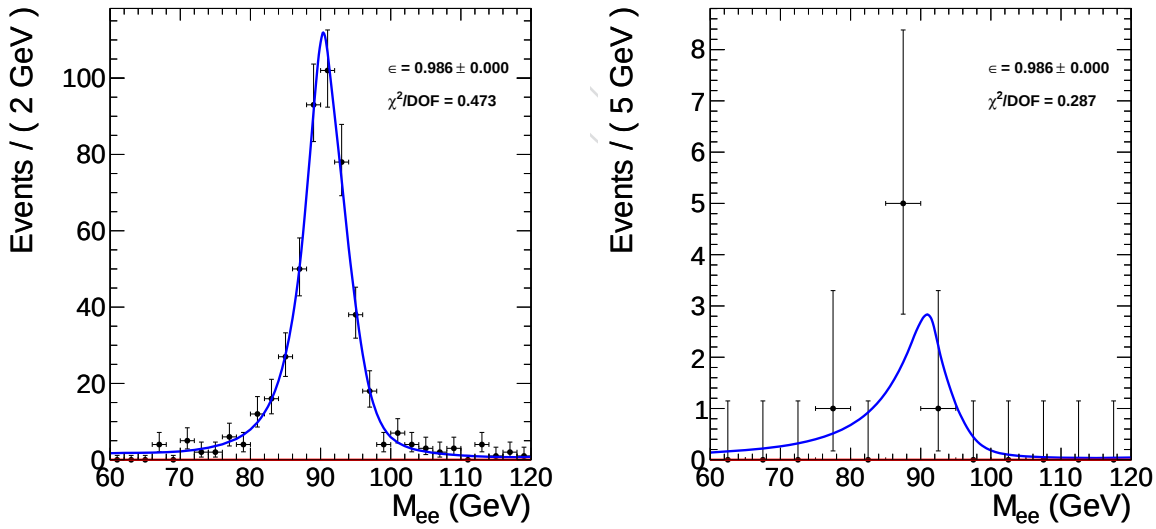

(a) (b)

Figure 24: The passing (a) and failing (b) fits for the WP80→HLT step in the Ecal Barrel for electrons. The data is in black, background fit in red, and signal+background fit in blue.

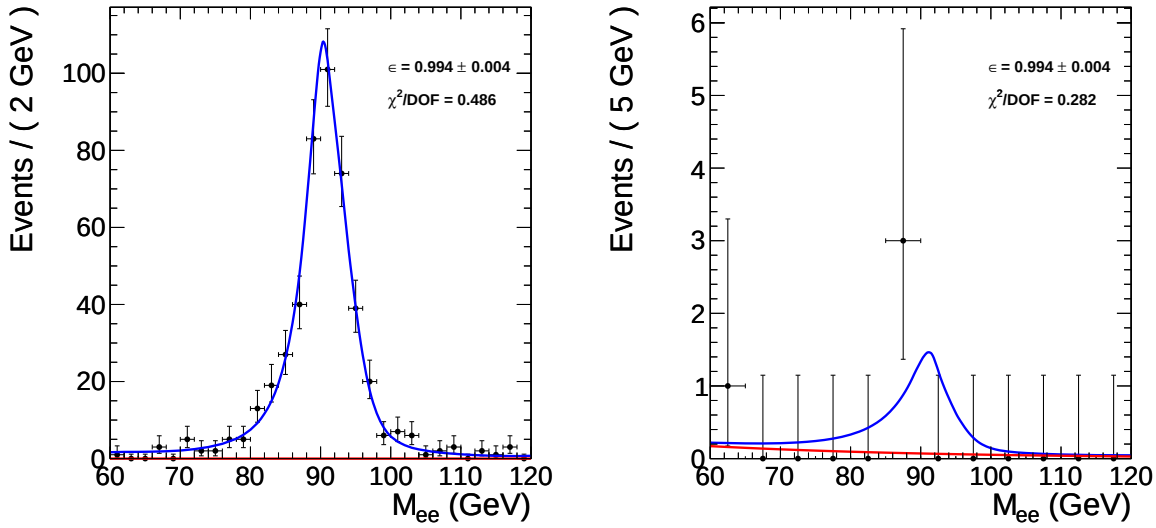

(a) (b)

Figure 25: The passing (a) and failing (b) fits for the WP80→HLT step in the Ecal Barrel for positrons. The data is in black, background fit in red, and signal+background fit in blue.

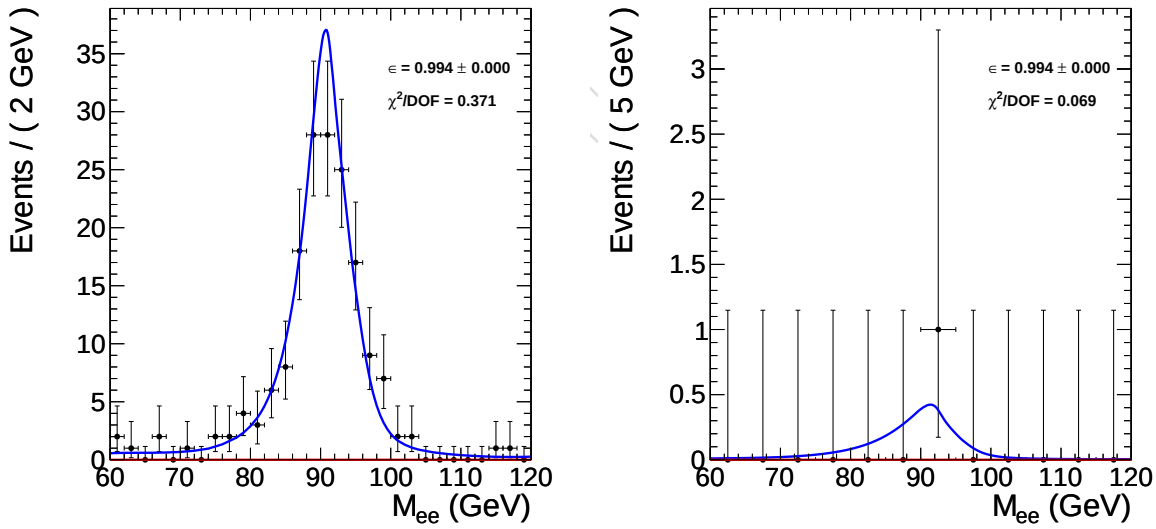

(a) (b)

Figure 26: The passing (a) and failing (b) fits for the WP80→HLT step in the Ecal Endcap for electrons. The data is in black, background fit in red, and signal+background fit in blue.

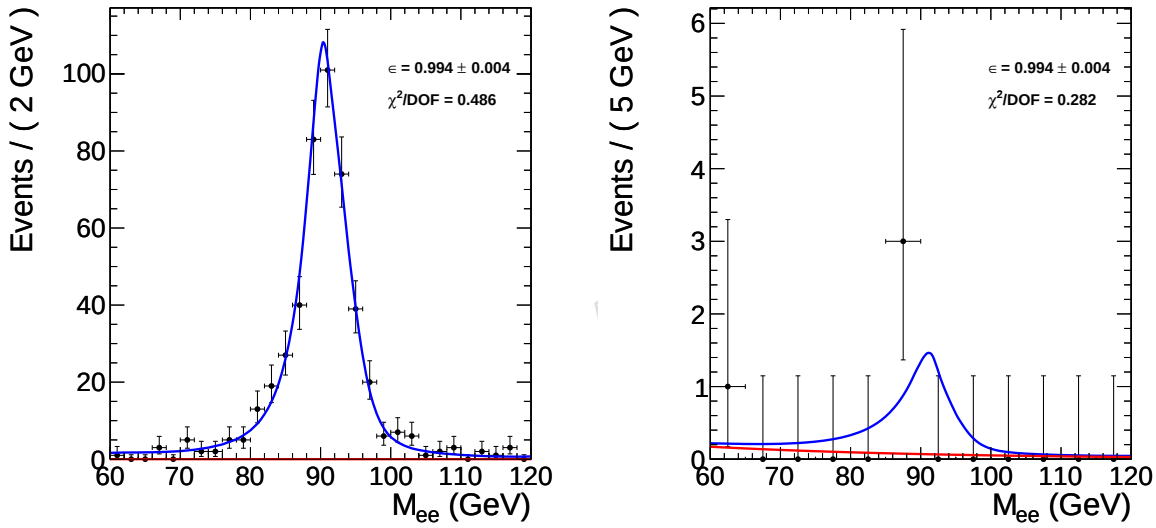

(a) (b)

Figure 27: The passing (a) and failing (b) fits for the WP80→HLT step in the Ecal Endcap for positrons. The data is in black, background fit in red, and signal+background fit in blue.